Food Chemistry 354 (2021) 129581

Contents lists available at ScienceDirect

Food Chemistry

journal homepage: www.elsevier.com/locate/foodchem

Effect of vacuum impregnated fish gelatin and grape seed extract on moisture state, microbiota composition, and quality of chilled seabass fillets

Xue Zhao [a,b], Lin Chen [a], Wanwisa Wongmaneepratip [a], Yun He [a], Lin Zhao [a], Hongshun Yang [a,b,*]

[a] Department of Food Science & Technology, National University of Singapore, Singapore 117542, Singapore
[b] National University of Singapore (Suzhou) Research Institute, 377 Lin Quan Street, Suzhou Industrial Park, Suzhou, Jiangsu 215123, PR China

ARTICLE INFO

Keywords:
Fish gelatin
Plant extract
Seafood
Microbiota composition
Moisture state
Vacuum infiltration
Spoilage
Protein

ABSTRACT

The effect of fish gelatin (FG) and grape seed extract (GSE) on microbiota composition and moisture state of fish was unexplored. Herein, this study aimed to evaluate the single and combined (FGG) effects on seabass during storage (4 °C) with assistant of vacuum impregnation and to elucidate the underlying preservative mechanism. As suggested by low-field NMR and magnetic resonance imaging, FGG-treated seabass presented higher water holding capacity by controlling transformation from immobilised to free water. Moreover, the total viable count and spoilage bacteria were reduced by > 1 log CFU/g as compared to the control. Changes in microbial flora analysed using high throughput sequencing further indicated that GSE contributed to the notably suppressed growth of *Pseudomonas*. Also, the accumulation of biogenic amines especially putrescine was decreased (over 0.5-fold) under the combination treatment as compared to the control ($P < 0.05$). The results suggest that FGG is promising for seabass preservation.

1. Introduction

Singapore has a small but thriving and increasingly important foodfish industry even with limited available sea space. Costal fish farms produce marine fish species including seabass. Asian seabass (*Lates calcarifer*), also known as barramundi, is one of the most important fishes for Singaporeans. Seabass is loved by multitudinous consumers because of its high protein, low fat and ideal fatty acids composition (high omega-3 and omega-6 fatty acids). However, for all these, seabass is highly perishable under the activities of relevant endogenous enzymes and microorganisms (Li, Peng, Mei, & Xie, 2020). Storage of seabass at 4 °C could preserve quality and freshness to some extents; however, the quality loss is inevitable and the fish flesh will eventually become inedible during chilled storage. With ever-increasing demand of consumers for fresh and safe seabass, it makes great sense to develop new preservation strategies to prolong the shelf life premised on high quality.

At present, many advanced technologies are being applied to fishery products, such as pulsed electric fields, active edible coating, high hydrostatic pressure, cold plasma, and irradiation (Zhao, de Alba, Sun, & Tiwari, 2019). Among them, natural edible coatings has attracted extensive attention from the fishery industry. The most important is that edible coatings have many advantages over other preservation strategies, for example, cost-effective, eco-friendly and can be safely consumed with packaged products (Yu et al., 2020). In particular, fish gelatin (FG) is a good resource to prepare edible coating since its biodegradability and good film-form property (Huang et al., 2019). FG has been regarded as a promising replacement of mammalian gelatin because of its similarity in functional properties and wide acceptance by vegetarians, halal and kosher. Moreover, Hanani, Roos, & Kerry (2012) showed that FG provided superior oxygen barrier as compared to pork gelatin and beef gelatin. However, the consideration of FG-based coating is its limited water resistance, thus it is somewhat sensitive to moisture. For the purpose of improving FG failing characteristics, some attempts have been made, for example, by the combination with polyphenols to form crosslinking (Huang et al., 2019).

Grape seed extract, is considered as a suitable source as it contains high levels of polyphenols. GSE has been generally recognised as a safe additive certified by the Food and Drug Administration. Relevant research have demonstrated that, GSE could not only retard the oxidative spoilage of tilapia fillets (Zhao et al., 2019), but also inhibited the survival of pathogenic bacteria (e.g., *Listeria monocytogenes*) on shrimp during storage (Zhao, Chen, Zhao, He, & Yang, 2020). However, the

* Corresponding author at: Department of Food Science & Technology, National University of Singapore, Singapore 117542, Singapore.
E-mail address: fstynghs@nus.edu.sg (H. Yang).

https://doi.org/10.1016/j.foodchem.2021.129581
Received 5 November 2020; Received in revised form 7 February 2021; Accepted 6 March 2021
Available online 15 March 2021

effects of combined GSE and FG coating on various spoilage bacteria in seabass are poorly understood, not to mention the influence on dynamic changes in microbiota composition on seabass fillets during chilled storage.

For practical application, edible coatings should present good adhesion ability. The most commonly used techniques to apply these coatings are dipping and spraying (Ju et al., 2019). However, the major disadvantages are that the coating efficiency is low and coating does not cling to the food surface. In this study, we applied vacuum impregnation (VI) to facilitate the coating process to satisfy highly-effective practical requirement. VI is a unit operation that affects the porous structures of foods and thus accelerates the two-way mass transfer between food matrix and impregnation solution. Nowadays, it has been widely applied in food industry to enrich food with various desirable compounds, e.g., cryoprotectants, anti-browning and antioxidant agents (Nian, Cao, Cai, Ji, & Liu, 2019; Zhao et al., 2019). The principle of VI was attributed to hydrodynamic mechanism and deformation-relaxation phenomena where pressure reduction and subsequent restoration of atmospheric pressure are the major driving forces (Yılmaz and Ersus Bilek, 2018).

The objective of the present study was to evaluate the effect of VI-introduced FG, GSE and their combination coatings on seabass fillets during 12-day storage. The changes in moisture state and water dynamics of chilled seabass fillets during storage at 4 °C were determined. Furthermore, to better understand of fish spoilage process and elucidate the underlying preservative mechanism, microbial enumeration was used to characterise the variations of predominant spoilage bacteria in seabass fillets while high-throughput sequencing was conducted to monitor the microbial composition and its changes during chilled storage. Lastly, selected physicochemical (biogenic amines) and colour qualities were tested.

2. Materials and methods

2.1. Preparation of edible coating solutions

Tilapia (*Oreochromis niloticus*) FG (200 bloom) was obtained from Jiangxi Kesheng Organism Co., Ltd (Jiangxi, China) while GSE was acquired from Tianjin Jianfeng Natural Product Co., Ltd (Tianjin, China). The preparation procedure of FG (4%, w/v) solution comprised the following steps: soaking FG in sterile deionised (DI) water; swelling FG at 4 °C overnight; heating FG solution at 60 °C for 30 min till it was totally homogenised. GSE solution (0.5%, w/v) was prepared by dissolving GSE in sterile DI water and homogenised using a magnetic stirring. The combined FG-GSE solution (abbreviated to FGG) was obtained by adding GSE into melted FG solution and then homogenising the mixture by magnetic stirring. The final concentration FG and GSE were 4% (w/v) and 0.5% (w/v), respectively. The chemical structures of FG, GSE and FGG were analysed using Fourier transform infrared (FTIR) spectroscopy (Sow, Toh, Wong, & Yang, 2019). The lyophilised samples (3 mg) were ground with 100 mg potassium bromide, pressed into a sheet and scanned with a Spectrum One FTIR spectrometer (PerkinElmer, Waltham, MA, USA) from 4000 to 450 cm^{-1}.

2.2. Preparation of seabass fillets

Live seabass (500 ± 50 g) was sacrificed with unnecessary parts (head, bone, and skin) removed and filleted at a local seafood market in Singapore. The seabass fillets were packaged in an ice box and then transported to our laboratory within one hour. After washing with sterile DI water, seabass fillets were further cut into 1 cm thick pieces weighting approximately 10 g.

VI was conducted in a jacketed chamber connected to a vacuum controller (IKA VC10, Guangzhou, Guangdong, China). Seabass fillets were fully immersed in the beakers containing different coating solutions at a mass ratio of 1: 3. The general VI procedure was conducted by following Zhao, Wu, Chen, and Yang (2019): 15-min vacuum pressure of 5 kPa; restoration to atmospheric pressure in 10 s. After VI processing, the seabass fillets were drained in a ventilated sterile biosafety cabinet (Esco Class II, Type A2, E-Series, Esco Micro Pvt. Ltd., Singapore) for 10 min. The treatment with sterile DI water was conducted simultaneously as a control. All the prepared samples were kept in a sterile bag and stored at 4 °C for 12 days. Fresh seabass fillets before treatment were also analysed (day 0).

2.3. Determination of moisture state

2.3.1. Low-field nuclear magnetic resonance (LF-NMR) analysis

The moisture distributions were determined using a LF-NMR analyser (NMI20-060H, Niumag Analytical Instrument Corporation, Suzhou, China) with a proton frequency of 21 MHz at 32 °C (Nian, Cao, Cai, Ji, & Liu, 2019). Seabass fillet was cut into 1.5 × 1 × 1 cm^3 block and then put in a 15 mm × 20 cm nuclear magnetic tube. The transverse relaxation (T_2) was tested with τ-value time analysis software (Niumag Analytical Instrument Corporation). T_2 was determined by Carr-Purcell-Meiboom-Gill sequence with a time delay between 90° pulse and 180° pulse (τ value) of 150 μs. Data from 8,000 echoes were obtained from 4 scans. The repetition time between consecutive scans was set as 3.5 s and each measurement was implemented for 5 times. T_2 distributions were obtained using MultiExp Inv analysis software.

2.3.2. Magnetic resonance imaging (MRI)

Proton density weighted image of seabass samples was obtained by a LF-NMR analyser (NMI20-060H, Niumag Analytical Instrument Corporation, Suzhou, China) with a spinecho sequence. The scanning protocol was set as follows: FOV Read 80 mm, FOV Phase 80 mm, read size 256, phase size 192, slice width 3 mm and slice 2 mm. Proton density weighted imaging echo time was 20 ms while repetition time was 2000 ms (Nian, Cao, Cai, Ji, & Liu, 2019). Preliminary process of proton density image was conducted using the Version 1.0 software of Niumag NMR imaging system.

2.3.3. Analysis of centrifugal loss

The centrifugal loss was determined based on the method described in a previous study (Zhang et al., 2019). Minced muscle weighed appropriately 5 g (W_1) was wrapped in filter paper and centrifuged for 15 min (4000 × *g*, 4 °C). The remaining seabass fillet after centrifuging was weighed as W_2. The centrifugal loss was calculated as the ratio of the lost weight to total initial weight.

2.3.4. Analysis of drip loss

The drip loss of seabass fillets during storage was determined based on the method described in a previous study (Zhao et al., 2019). The drip loss was calculated as the percentage of weight change on sampling day as compared to the weight on day 0 (after coating).

2.4. Microbial analysis of seabass fillets

2.4.1. Microbial enumeration

Microbial enumeration of total viable counts (TVC), *Pseudomonas*, H_2S-producing bacteria and *Aeromonas* were analysed based on the method as described in previous papers (Lou, Zhai, & Yang, 2021; Zhuang et al., 2019). Ten grams of fish were homogenized with sterile 0.85% saline solution (90 mL) using stomacher (Masticator Stomacher, IUL Instruments, Germany) for 3 min. After serial dilution, 100 μL of diluent was spread on the Plate Count Agar. TVC was determined after incubation at 37 °C for 2 days and expressed as log colony-forming unit (CFU)/g. *Pseudomonas* and H_2S-producing bacteria were incubated at 25 °C on *Pseudomonas* agar base added with C.F.C supplement and iron agar medium, respectively, for 48 h. *Aeromonas* counts were enumerated after incubation at 30 °C for 48 h on *Aeromonas* medium base including *Aeromonas* Selective Supplement.

2.4.2. Illumina-MiSeq high throughput sequencing

Ten grams of fish samples were mixed with 20 mL sterile saline solution and shaken for 20 min. The mixture was then centrifuged at 200 × *g* for 5 min, and the sediment was discarded. The supernatant was further centrifuged at 10,000 × *g* for 10 min, and the bacterial pellets were collected. DNA of bacteria was extracted using a bacterial DNA isolation kit (Bomad Biological Technology Co., Ltd., Beijing, China) based on a method described in a previous study (Zhuang et al., 2019). The V3–V4 region of the bacteria 16S ribosomal RNA gene of each sample was amplified using polymerase chain reaction (PCR) with primers 341F 5′-CCTACGGGNGGCWGCAG-3′ and 805R 5′-GACTACHVGGGTATCTAATCC-3′. PCR was conducted in a final volume of 20 μL reaction mixture containing 0.8 μL primer 341F (5 μM), 0.8 μL primer 805R (5 μM), 10 μL template DNA, 4 μL 5 × FastPfu Buffer, 0.4 μL FastPfu Polymerase, 2 μL dNTPs (2.5 mM), and 2 μL ddH_2O. The PCR program was set as follows: 95 °C for 2 min, 25 cycles at 95 °C for 30 s, 55 °C for 30 s, 72 °C for 30 s and 72 °C for 5 min. After that, the obtained amplicons were extracted using 2% agarose gels. The AxyPrep DNA Gel Extraction Kit was used for purification (Axygen Biosciences, Union City, CA, USA) while QuantiFluor™-ST (Promega, Madison, Wisconsin, USA) was used for further quantification. In the end, amplicons were pooled together in equimolar for paired-end sequenced (2 × 300 bp) on an Illumina MiSeq platform. The raw reads were stored in NCBI Sequence Read Archive database.

2.5. Determination of biogenic amines

The extraction and derivatisation of biogenic amines from fish samples were according to the method described by Li et al. (2020). Three grams of mince fish were homogenised with 6 mL cold perchloric acid (PCA, 0.6 M) and centrifuged at 10,000 × *g* for 5 min. The sediments were washed for two times under the same condition. The supernatants were combined and adjusted to a final volume of 20 mL with 0.6 M PCA. The extracts were kept at –20 °C prior to derivatisation and further analysis.

The extracts of biogenic amines were identified and quantified using high-performance liquid chromatography (HPLC, Water 2695 Alliance system, Milford, MA, USA) equipped with a Luna C18 column (150 mm, 4.6 mm; Phenomenex, Torrance, CA, USA) and a UV detector at 254 nm. The liquid chromatography conditions were set as follows: flow rate was 0.8 mL/min, injection volume was 10 μL, mobile phase A was 0.1 mol/L ammonium acetate and mobile phase B was 100% acetonitrile. The elution gradient was: 0 min, 50% B; 25 min, 90% B; 35 min, 90% B; and 45 min, 50% B. The retention time and peak area of samples were compared with that of standards (Sigma-Aldrich, Singapore).

2.6. Colour measurement

Changes in lightness (L*), redness-greenness (a*); blue-yellowness (b*) of seabass fillets were analysed using a Minolta Colorimeter CM-3500d (Konica Minolta, Tokyo, Japan) (Zhao, Chen, Zhao, He, & Yang, 2020). Colour difference (ΔE) between non-treated fresh seabass and treated-samples on day 0 (within 1 h after coating), 3, 6, 9, and 12 was further calculated using the following equation:

$$\Delta E = \sqrt{(\Delta L^*)^2 + (\Delta a^*)^2 + (\Delta b^*)^2} \quad (1)$$

2.7. Statistical analysis

All measurements were conducted in triplicate independently. Experimental data were analysed statistically using two-way analysis of variance (ANOVA) and comparisons between different groups were conducted with the least significant difference (LSD) method by IBM SPSS Statistics 25 (International Business Machines Co. Armonk, NY, USA). The significance level was set as 0.05.

3. Results and discussion

3.1. Changes in moisture state

3.1.1. LF-NMR

Fig. 1A presents the changes in relaxation signal intensity at the initial, middle and final stages of storage under different treatments. Based on T_2 transverse relaxation time, three types of water were observed, including bound water ($0 < T_{2b} < 1 < T_{21} < 10$ ms), immobilised water ($10 < T_{22} < 100$ ms) and free water ($100 < T_{23} < 1000$ ms). Generally, both T_{2b} and T_{21} refer to water tightly bound to macromolecules (e.g., protein), T_{22} represents immobilised water being trapped in the complex network of myofibrillar proteins while T_{23} corresponds to free water that exists inside the cell space and could be removed easily (Li, Li, & Zhang, 2018).

During refrigerated storage, T_{2b} and T_{21} fluctuated in the range of 0.12–0.40 and 1.06–2.03 ms, respectively, with no significant differences ($P > 0.05$). T_{22} of all samples continued to increase from the initial till the end of storage. Similarly, T_{23} showed overall upward tendency in all samples and reached the maximum values of 748.81, 541.59, 636.82, and 499.45 ms on day 12 for the control, FG, GSE and FGG groups, respectively. GSE showed limited effect on controlling the increase of T_{23} and it worked only at the end of the storage. The inhibitory effect of GSE on the water release of seabass fillets might be contributed to its action against muscle denaturation and myofibril structures destruction (Zhang et al., 2019). Furthermore, it is worth noticing that the addition of FG especially when combined with GSE, inhibited the prolongation of T_{22} and T_{23} during the whole storage period, suggesting the alterations of water dynamics in seabass fillets. Generally, extended relaxation time meant increased mobility of water and the potential to transform to the next water form in the order from bound water, immobilised water to free water (Pearce, Rosenvold, Andersen, & Hopkins, 2011). It has been reported that FG was capable of holding water tightly inside meat products due to its abundant content in hydrophilic amino acids (Jridi et al., 2015). Thus, it could possibly be inferred that FGG treatment modified the water dynamics and further inhibited the possible water release in seabass fillets which mainly owed to FG.

The ratio of bound water ($P_{2b} + P_{21}$) was < 5% in all groups (Fig. 1B) and hardly affected by either treatment or storage time, indicating a tight bounding force between protein and water. It has been verified that, bound water showed a reduced mobility only under severe mechanical and/or physical stresses (Zhang et al., 2017). Immobilised water accounted for the largest proportion of the total water, reaching up to over 90%. With the increase of storage time, the ratio of immobilised water (P_{22}) experienced a gradual decline no matter what kind of treatment was applied. The most prominent decline in P_{22} was observed in the control group at the final stage of storage. As a comparison, the FGG group had the highest P_{22} during storage as compared to other groups. It has been demonstrated that water existed in highly organised myofibril network transformed to free water depending on the destroying degree of myofibril (Albertos et al., 2019). Owing to the capability of FG and GSE in retarding the myofibril degradation (Zhao et al., 2019), this combined treatment could hold immobilised water and further inhibit the migration from immobilised form into free water, which were in line with our findings on inhibited extension of T_{22}.

Free water is retained via capillary force between water and its surroundings, significant increase in free water (P_{23}) was observed in all groups along with the process of storage due to shrinkage of myofibrillar proteins ($P < 0.05$) (Zhang et al., 2017). Aside from this, the control group experienced a drastic rise in P_{23} from 1.15% on day 0 to 5.14% on day 12, indicating massive loss of immobilised water as well as accumulation of free water. On the contrary, the FGG treatment restrained the increase in P_{23}. It has been illustrated that mobilised free water presenting in extra-myofibrillar space was the potential drip in meat structures, thus increased P_{23} led to the poor water holding capacity in seabass fillets (Bertram, Purslow, & Andersen, 2002). Taken conjointly,

(A)

Group	T_{2b} (ms)	T_{21} (ms)	T_{22} (ms)	T_{23} (ms)
d0	0.12±0.02^{a}	1.25±0.21^{ab}	34.49±3.85^{a}	333.13±26.19^{a}
Control-d6	0.15±0.03^{a}	1.72±0.33^{bcd}	47.69±3.35^{bcdc}	460.59±40.94^{cdc}
FG-d6	0.16±0.02^{ab}	1.46±0.17^{abc}	40.55±5.77^{abc}	391.71±28.30^{abc}
GSE-d6	0.18±0.04^{ab}	1.59±0.25^{abcd}	43.98±4.89^{abcd}	424.76±30.72^{bcd}
FGG-d6	0.27±0.06^{b}	1.06±0.11^{a}	37.40±2.98^{ab}	361.23±33.78^{ab}
Control-d12	0.21±0.07^{ab}	1.59±0.26^{abcd}	60.80±7.22^{f}	748.81±46.69^{g}
FG-d12	0.12±0.04^{a}	2.03±0.34^{d}	51.71±4.14^{def}	541.59±42.48^{e}
GSE-d12	0.40±0.09^{c}	1.87±0.24^{cd}	56.07±4.94^{ef}	636.82±36.81^{f}
FGG-d12	0.14±0.05^{a}	1.15±0.13^{a}	48.22±3.02^{cdc}	499.45±49.22^{dc}

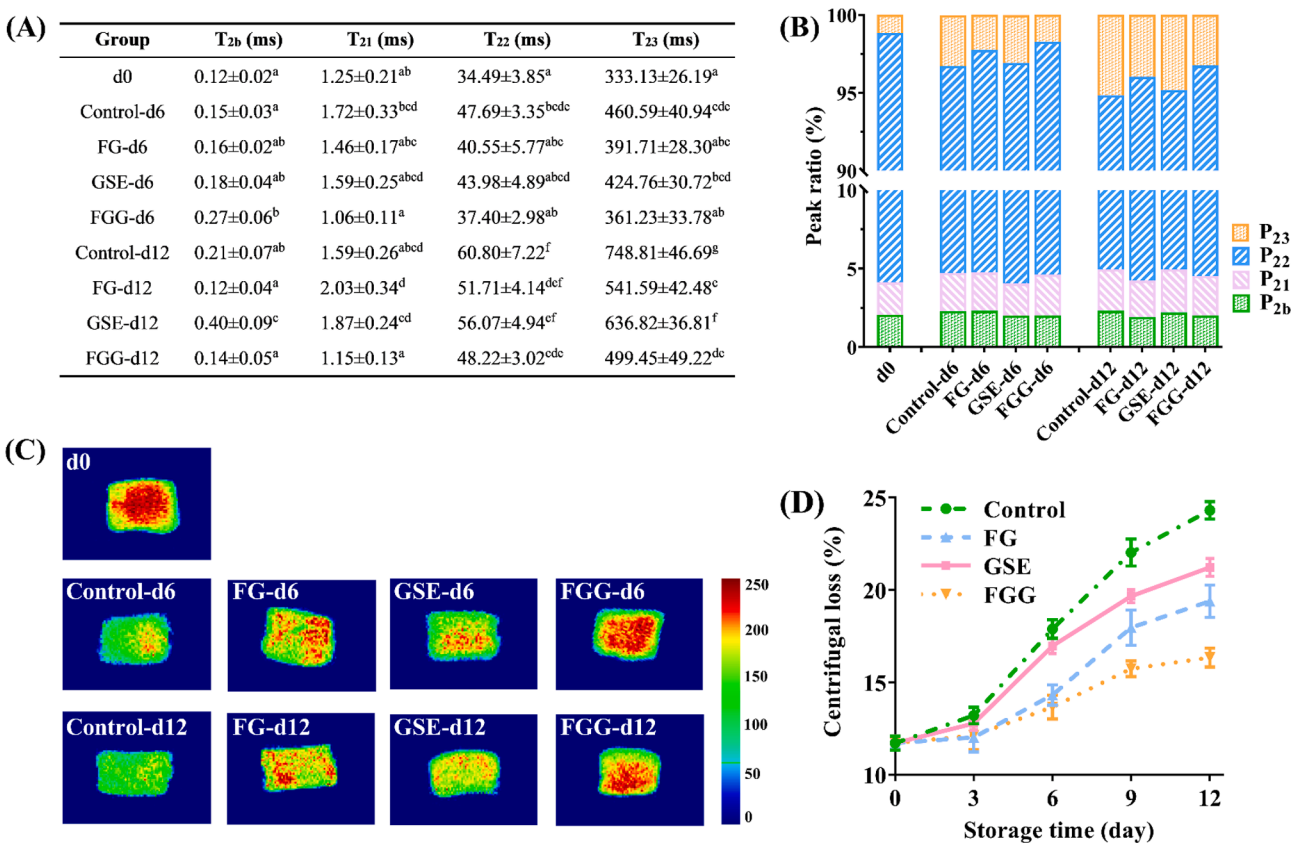

Fig 1. Changes of LF-NMR relaxation time (A), percentage of each relaxation component (B) in seabass fillets, magnetic resonance imaging (C) and centrifugal loss (D) during storage at 4 °C. Notes: FG: fish gelatin; GSE: grape seed extract; FGG: the combination of FG and GSE. d0, d6, d12 suggested that samples were stored for 0 (untreated), 6 and 12 days, respectively. Values with different lowercase letters in the same column indicate significant differences ($P < 0.05$).

the effect of FGG on water migration (retarded extension of T_{22} and T_{23}, inhibited increase of P_{23} and reduction of P_{22}) also verified its ability in maintaining the water holding capacity of seabass fillets.

3.1.2. *Visualisation of water distribution by MRI in seabass fillets*

As a fast and non-invasive technique, MRI has been utilised to visualise the internal structure of food samples. It can not only determine their water distribution, but also visualise the structural changes during processing. Proton density weighted figures, as presented in Fig. 1C, afforded valuable information on the internal changes of water state in the seabass fillets during storage. In these pseudo-colour images, red colour means high density of H proton while blue colour signifies low density of proton (Zhou, Li, Fang, Mei, & Xie, 2020). It can be easily observed that proton density decreased rapidly as storage went on in the control group. As a comparison, the samples treated by FG rather than GSE showed higher quantitative intensity, suggesting FG addition could sustained the water holding capacity of seabass fillets (Nian, Cao, Cai, Ji, & Liu, 2019). Moreover, the FGG group was much redder as compared to other groups under the same storage time, demonstrating that the FG-based coating containing bioactive GSE was the most effective strategy for quality maintenance of seabass fillets during chilled storage. In general, the MRI results were in line with the variations of LF-NMR transverse relaxation.

3.1.3. *Centrifugal loss of seabass fillets*

Extrinsic forces such as centrifugal force can cause release of free and immobilised water from muscle (Pearce et al., 2011). As shown in Fig. 1D, upward tendencies of centrifugal loss were observed in all treatments from the initial value of 11.71% to 24.31%, 19.39%, 21.22%, and 16.34% on day 12 in the control, FG, GSE and FGG groups, respectively. The significant growth of centrifugal loss further indicated the decreased water holding capacity of seabass fillets during storage ($P < 0.05$). As the proteolysis process of structural proteins took the major responsibility for protein-bound water release (Zhang et al., 2019), reduced water holding capacity was more pronounced in the control group. Zhang and Xie (2019) also reported that the aggregation and denaturation of myofibrillar proteins were responsible for the increased centrifugation loss.

3.1.4. *Drip loss of seabass fillets*

Table S1 shows the drip loss of seabass fillets during storage. As presented, there was a significant and rapid increase of drip loss in all treated groups throughout chilled storage ($P < 0.05$), from 1.75% to 2.83% on day 3 to 5.08%–7.55% on day 12. The drip loss of fish muscle has been observed to be attributed to the accelerated protein degradation (Zhao et al., 2019). Moreover, significant differences were observed among four groups throughout storage period. FGG showed better preservation effect with drip loss of 5.08% at the end of the storage as compared with other groups, especially the control (7.55%) and GSE (7%) groups during the whole storage period.

3.2. *Microbial analysis of seabass fillets*

3.2.1. *Microbial survival*

The initial TVC in seabass fillets was 3.89 log CFU/g (Fig. 2A). With the increase of storage time, TVC in all groups increased with varied rates. There was no significant difference between the control and FG groups ($P > 0.05$) and a rapid increase in both groups was observed since day 6. The TVC of the control and FG groups kept increasing during storage and reached 7.24 and 7.05 log CFU/g on day 9, respectively, higher than the maximum edible limit (7 log CFU/g) for fish (Chaijan, Panpipat, Panya, Cheong, & Chaijan, 2020). However, addition of GSE

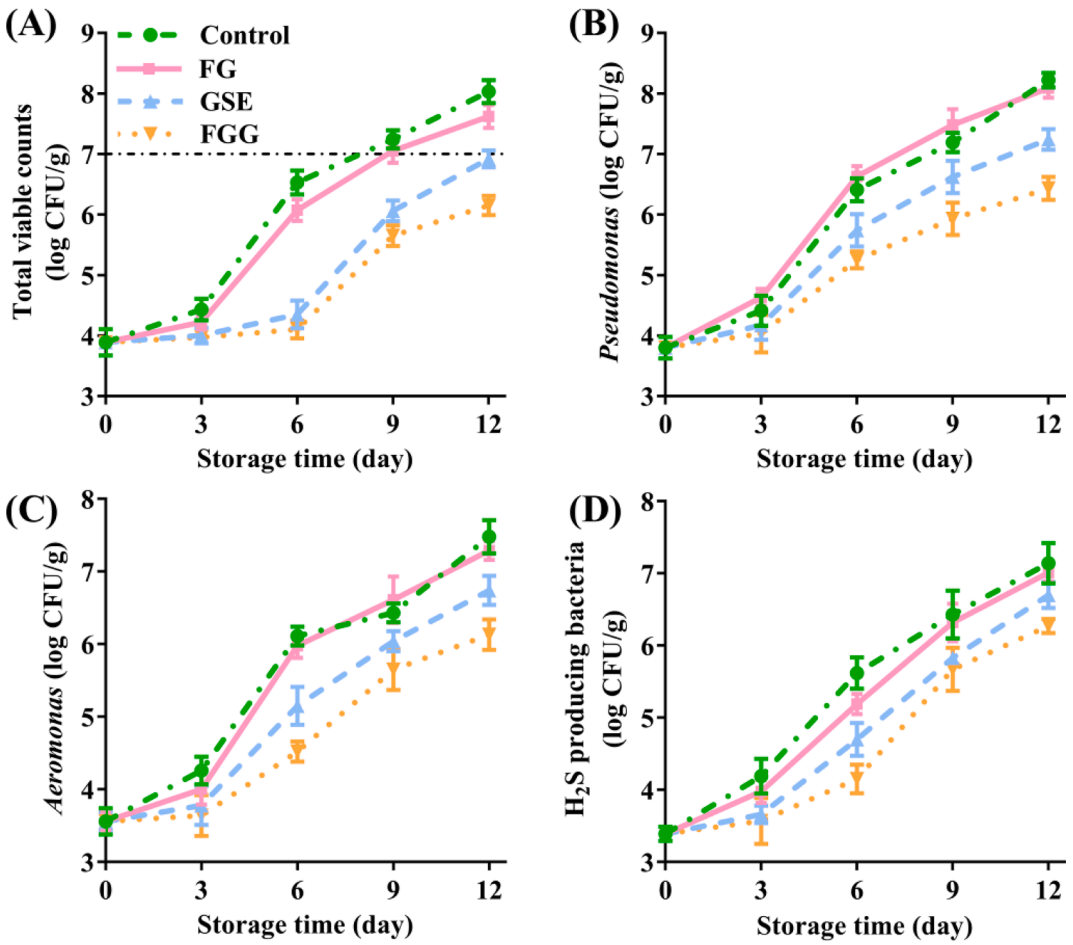

Fig 2. Changes in total viable counts (A), *Pseudomonas* (B), *Aeromonas* (C), and H_2S-producing bacteria (D) in seabass fillets during storage at 4 °C. Notes: FG: fish gelatin; GSE: grape seed extract; FGG: the combination of FG and GSE.

especially when facilitated with FG showed a notable inhibitory effect on the growth of TVC. Till the end of storage, the TVC values in GSE and FGG groups were still within the acceptable level, indicating the seabass fillets were under relatively good status. These results demonstrated the antimicrobial capability of GSE which were in line with previous studies (Li et al., 2020; Zhao et al., 2019). Several antibacterial mechanisms of GSE have been proposed. For example, the hydrophobic phenolic components could interact with bacterial surface structures and lipopolysaccharides resulting in the reduction of membrane stability (Olatunde & Benjakul, 2018). The inhibition effect of GSE on the growth of *Staphylococcus aureus* was related to the suppression of a key enzyme (dihydrofolate reductases) that involving in the biosynthesis of several vital biomolecules (Memar et al., 2019). Moreover, GSE was reported to inhibit the survival of *L. monocytogenes* by blocking glycolysis and amino acid metabolism (Zhao, Chen, Wu, He, & Yang, 2020).

Preponderant populations in spoiled fish are mainly gram-negative bacteria, for example, *Pseudomonas*, *Aeromonas* and *Shewanella* (the primary H_2S-producing bacteria) (Fig. 2B–D). The initial populations of *Pseudomonas*, *Aeromonas* and H_2S-producing bacteria in seabass fillets were 3.56, 3.80 and 3.39 log CFU/g, respectively. During chilled storage, all these spoilage bacteria experienced similar growth tendencies as TVC. *Pseudomonas* in the control and FG groups increased at a high rate, exceeding 8 log CFU/g on day 12 while *Aeromonas* and H_2S-producing bacteria counts were only around 7 log CFU/g at the end of storage. This result suggested that *Pseudomonas* was more predominant than *Aeromonas* and H_2S-producing bacteria in the later stage of seabass storage, which was in accordance with previous observations (Arfat, Benjakul, Vongkamjan, Sumpavapol, & Yarnpakdee, 2015). Moreover, significant reductions in *Pseudomona* (> 1 log CFU/g) were observed in GSE-based groups as compared with the control and FG groups. The GSE treatment especially when combined with FG was more effective in inhibiting *Pseudomona* than *Aeromonas* and H_2S-producing bacteria.

3.2.2. *Microbiota composition*

To obtain a more profound insight into microbial variations on seabass fillets during refrigeration, the succession of microbial flora was further analysed. A total number of 534,326 valid reads were obtained after quality screening through the Illumina sequencing of bacterial 16S rRNA gene (Table 1). The coverage values of all groups exceeded 0.998, suggesting that the vast majority of bacterial phylotypes were detected and identified with high enough sequencing depths. Decrease in Shannon and Simpson values meant that the community diversity of seabass fillets at later stage of storage was less than that at the initial state. In addition, clear decreases in ACE and Chao were observed as storage time went on, which further indicated the reductions of microbial community richness over time.

Fig. 3A shows the microbiota composition as well as the relative abundance at genus-level in seabass fillets at the initial, middle and final stage of storage. Relative abundance of genera in seabass fillets at the genus-level showed that *Brochothrix*, *Psychrobacter* and *Acinetobacter* were the most predominant genera, accounting for 25.41%, 20.49%, and 14.74% of all microbiota, respectively, followed by *Photobacteria* with a proportion of 10.16%. Such organisms are commonly present in fresh fish (Fraser & Sumar, 1998). During the period of fish storage, microbiota composition changed remarkably and only part of bacteria, namely those spoilage bacteria, took part in the decay process. The

Table 1
Alpha diversity indices of microbiota in seabass fillets during storage at 4 °C.

Group	Read number	OTUs	Shannon	Simpson	Chao	ACE	Coverage ($\times 10^{-2}$)
d0	56217 ± 612^{bcd}	283 ± 1^{a}	2.37 ± 0.05^{a}	0.68 ± 0.04^{a}	323.25 ± 14.03^{a}	340.47 ± 10.50^{a}	99.88 ± 0.13^{a}
Control-d6	78221 ± 299^{ef}	246 ± 4^{b}	1.45 ± 0.06^{bc}	0.32 ± 0.03^{d}	303.11 ± 8.49^{b}	310.98 ± 5.58^{b}	99.92 ± 0.17^{a}
FG-d6	53678 ± 607^{bc}	232 ± 18^{b}	1.36 ± 0.24 ^{cd}	0.39 ± 0.02^{c}	305.02 ± 4.86^{b}	302.81 ± 18.82^{b}	99.87 ± 0.03^{a}
GSE-d6	48074 ± 1768^{a}	233 ± 11^{b}	1.65 ± 0.06^{b}	0.54 ± 0.08^{b}	308.04 ± 5.84^{b}	295.09 ± 3.30^{bc}	99.81 ± 0.02^{a}
FGG-d6	52668 ± 3612^{b}	239 ± 16^{b}	1.57 ± 0.25^{bc}	0.63 ± 0.02^{a}	296.88 ± 3.77^{b}	304.13 ± 9.94^{b}	99.90 ± 0.01^{a}
Control-d12	58106 ± 876^{d}	70 ± 4^{f}	1.19 ± 0.15^{de}	0.15 ± 0.05^{f}	91.11 ± 7.57^{f}	92.74 ± 4.71^{f}	99.93 ± 0.01^{a}
FG-d12	65358 ± 2241^{e}	177 ± 11^{c}	0.81 ± 0.04^{f}	0.19 ± 0.03^{ef}	136.04 ± 6.32^{d}	274.34 ± 10.07^{d}	99.89 ± 0.02^{a}
GSE-d12	56801 ± 1162 ^{cd}	141 ± 5^{d}	0.98 ± 0.09^{ef}	0.20 ± 0.02^{ef}	172.27 ± 3.16^{c}	232.10 ± 6.65^{e}	99.88 ± 0.03^{a}
FGG-d12	65203 ± 1655^{e}	94 ± 6^{e}	0.80 ± 0.02^{f}	0.24 ± 0.02^{e}	123.16 ± 5.24^{e}	283.53 ± 13.62 ^{cd}	99.87 ± 0.01^{a}

Notes: FG: fish gelatin; GSE: grape seed extract; FGG: the combination of FG and GSE. d0, d6, d12 suggested that samples were stored for 0 (untreated), 6 and 12 days, respectively. OTUs: operational taxonomic units; Shannon: the Shannon index of community diversity; Simpson: the Simpson index of community diversity; Chao: the Chao1 estimator of community richness; ACE: the ACE estimator of community richness; Coverage: the good's community coverage. Values with different lowercase letters in the same column indicate significant difference ($P < 0.05$).

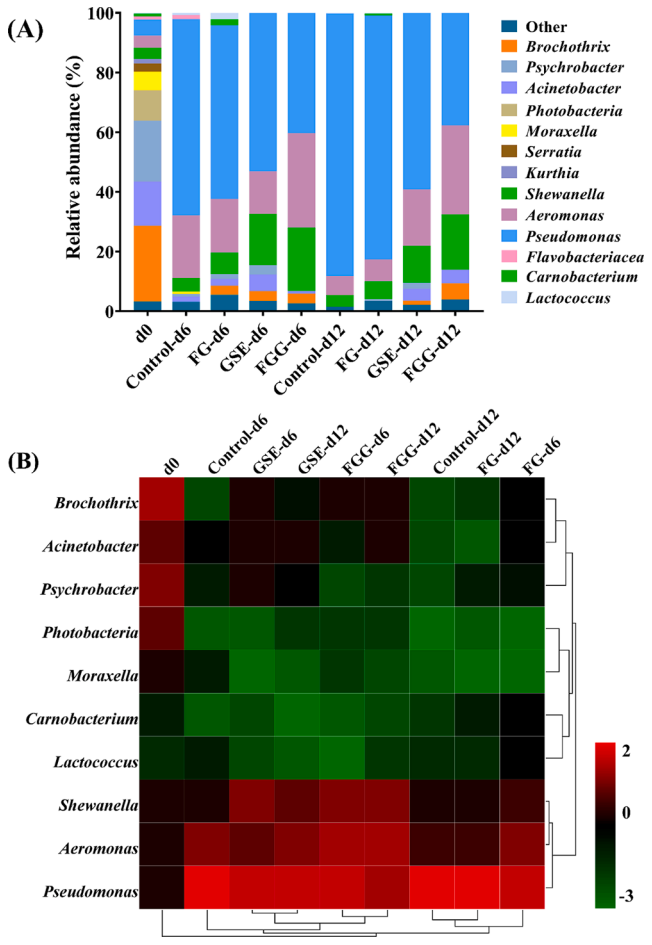

Fig 3. Composition and relative abundance of microbiota at the genus level (A); and community heatmap at the genus level (B). Notes: FG: fish gelatin; GSE: grape seed extract; FGG: the combination of FG and GSE. d0, d6, d12 suggested that samples were stored for 0 (untreated), 6 and 12 days, respectively.

growth and relative abundance of spoiler (e.g., *Pseudomonas*, *Aeromonas*, *Shewanella* and *Acinetobacter*) tended to increase and then caused spoilage during refrigerated storage of fish fillets (Cao et al., 2020).

On day 6, the control sample was close to decay (TVC: 6.53 log CFU/g). *Pseudomonas*, *Aeromonas* and *Shewanella* with a relative abundance of 65.8%, 21.01%, and 4.49%, respectively, became the top three genera. It became completely decayed on day 12, and its microbiota was mostly comprised of *Pseudomonas* (88.01%), followed by *Aeromonas* (6.32%) and *Shewanella* (3.89%). The microbial flora of FG-treated group was quite similar to that of the control group, manifesting FG alone showed negligible antimicrobial effect, which was in accordance with the TVC result and a previous study (Zhao et al., 2019). *Pseudomonas* have a quite high spoilage activity as compared to other spoilage bacteria (Fraser & Sumar, 1998), thus the dramatic increase in *Pseudomonas* in the control and FG groups during storage indicated a more rapid spoilage process as compared to the GSE and FGG groups.

As for the GSE group, its microbiota composition was quite different from the control and FG groups when it reached a close-to-spoilage state on day 12 (TVC: 6.92 log CFU/g). Relative abundance of *Pseudomonas* accounted for only 59.13% of the total microbiota while a corresponding increase in both *Aeromonas* (18.92%) and *Shewanella* (12.40%) was observed. This result might possibly because GSE was effective in retarding the growth of *Pseudomonas* in seabass during storage, resulting in differential microbial community between different groups (Li et al., 2020). Moreover, it is worth noticing that GSE group experienced a moderate recovery in *Pseudomonas* from day 6 (53.16%) to day 12. This phenomenon further verified the increase of TVC at a relative higher rate at latter storage stage, suggesting that the antimicrobial efficiency of GSE decreased gradually in the later period of storage. As a comparison, the binary treatment showed higher and more lasting inhibitory effect on *Pseudomonas*, keeping reducing the relative abundance of *Pseudomonas* from 40.29% on day 6 to 37.66% on day 12. This could be explained since FG-based coating could sustain the release of GSE in a slow way, maintaining the seabass fillets in a GSE-rich condition during the whole process of storage (Cao et al., 2019; Zhao, Wu, Chen, & Yang, 2019).

What's more, the heatmap of the top 10 genera in seabass fillets was plot to visualise the composition and dynamic changes during chilled storage (Fig. 3B). The red/green colour with different levels of depth represents the relative abundance of the genus. The microbiota composition of fresh seabass fillets was the most abundant one as compared with other samples, with no specific genus became a clear dominant flora (Syropoulou, Parlapani, Bosmali, Madesis, & Boziaris, 2020). However, the stored seabass was mainly dominated by *Pseudomonas*, *Aeromonas* and *Shewanella* and their corresponding proportions were influenced by different treatments. Furthermore, the right and bottom sides of the heatmap also present genus clustering and group clustering, respectively, based on the similarity in genera abundance. Generally, the clustering analysis of different groups indicated that microbiota compositions of FGG group on day 6 and day 12 were similar to that of GSE-treated samples on day 6 and day 12 as compared to other groups. In the meantime, similar genera in the control and FG samples stored for 12 days were also drawn together. These results further indicated that it was GSE that contributed largely to inhibitory effect of FGG against spoilage bacteria during storage of seabass fillets.

3.3. Changes in biogenic amines

Generally, generation and accumulation of biogenic amines are caused by the protein hydrolysis, transamination of aldehydes and ketones, as well as microbial-induced amino acid decarboxylation is a common phenomenon during storage (Visciano, Schirone, Tofalo, & Suzzi, 2012). Table 2 exhibits the concentrations of six biogenic amines in seabass fillets during chilled storage, among which putrescine and cadaverine were considered as the major indicators for fish spoilage. As major off-flavour contributors of rotting fish, putrescine and cadaverine are transformed from ornithine and lysine with the action of corresponding bacterial decarboxylases (Latorre-Moratalla, Bover-Cid, Bosch-Fusté, Veciana-Nogués, & Vidal-Carou, 2014). In our study, the initial concentrations of putrescine and cadaverine were 0.96 and 1.58 mg/kg, respectively; both of them remained at relative low levels at the early stage of storage. A sharp rise in putrescine level was observed on day 6 in the control group, which was in accordance with the sudden increase of TVC. The addition of GSE, especially when combined with FG, significantly inhibited the accumulation of putrescine ($P < 0.05$).

Similar tendency was observed in cadaverine; however, it increased at a slower rate as compared to putrescine under the same condition. The levels of cadaverine increased continuously, reaching up to 4.86 (control group) and 3.94 (FG group) mg/kg at the end of storage, which were significantly higher than those in the GSE (2.91 mg/kg) and FGG (2.39 mg/kg) groups ($P < 0.05$). GSE is effective in retarding the formation of cadaverine, though to a less extent as compared to putrescine. The inhibitory effect of GSE on biogenic amines formation was mainly due to the antimicrobial effect of GSE. It has been reported that putrescine accumulation has a close relation with the activities of spoilage bacteria *Pseudomonas* while *Aeromonas* and *Shewanella* are more responsible for cadaverine production (Jia et al., 2019; Zhuang et al., 2019). Therefore, it might be reasonable to be draw the conclusion that GSE was more effective in inhibiting *Pseudomonas* than *Aeromonas* and *Shewanella*, which agreed with the microbial analysis results.

Regarding histamine, it is considered as a toxic biogenic amine as it is capable to induce allergies and immune system disorders (Biji, Ravishankar, Venkateswarlu, Mohan, & Gopal, 2016). It was not detected until day 3 in the control, FG and GSE groups, while it appeared on the sixth day in the FGG group with a low concentration (0.32 mg/kg). A moderate increase in histamine was observed in all four groups while GSE attenuated the production of histamine. The concentration of histamine remained at a safe level which was lower than 50 mg/kg, a maximum limit as suggested by the Food and Drug Administration. It is observed that spermidine had the highest initial concentration among all biogenic amines since it is a natural substance of living cells (Cao et al., 2020). Slow increase or even decrease changing trends of tyramine, spermidine and spermine during storage were observed, in the control and FG groups with no significant difference ($P < 0.05$). This was in accordance with a previous research conducted by Li et al. (2020). The FGG treatment maintained tyramine, spermidine and spermine at comparable levels as compared to the initial concentrations. The generation of biogenic amines depends on multiple elements, for instance, the precursors (as substrate) levels and bacterial activities (growth state, decarboxylase ability, etc.). Thus, the decrease of spermidine and spermine may be related to both limited precursor amino acids and bacteria with low activities (Lázaro, Monteiro, & Conte-Junior, 2020).

3.4. Changes in colour of seabass fillets during storage

Colour characteristics are important factors that reflect the quality of seafood products and affect consumers' acceptance. As shown in Table S2, there are significant differences in L*, a*, b* values of between different treatments (day 0, within 1 h after VI-assisted coating) ($P < 0.05$). FG resulted in the increased brightness while GSE was responsible for the rise in a* and b* since the original colour of GSE-based solutions were somewhat purplish-red. The influences of FG and phenolic extracts

Table 2
Changes in biogenic amines in seabass fillets during storage at 4 °C.

Biogenic amine (mg/kg)	Treatment	Storage time (day)				
		0	3	6	9	12
Putrescine	Control	0.96 ± 0.14^{Aa}	1.13 ± 0.03^{Aa}	3.49 ± 0.05^{Ba}	6.75 ± 0.25^{Ca}	16.51 ± 0.16^{Da}
	FG	0.96 ± 0.14^{Aa}	1.04 ± 0.06^{ABab}	2.32 ± 0.02^{Bb}	4.12 ± 0.24^{Cb}	15.41 ± 0.29^{Db}
	GSE	0.96 ± 0.14^{Aa}	1.05 ± 0.03^{Aab}	1.11 ± 0.06^{Ac}	2.76 ± 0.16^{Bbc}	9.96 ± 0.32^{Cc}
	FGG	0.96 ± 0.14^{Aa}	0.98 ± 0.07^{Ab}	1.03 ± 0.05^{Ac}	2.36 ± 0.29^{Ac}	6.74 ± 0.37^{Bd}
Cadaverine	Control	1.58 ± 0.03^{Aa}	1.90 ± 0.04^{Ba}	2.13 ± 0.20^{Ca}	3.14 ± 0.09 ^{Da}	4.86 ± 0.17^{Ea}
	FG	1.58 ± 0.03^{Aa}	1.75 ± 0.08^{Ab}	2.02 ± 0.12^{Bab}	2.70 ± 0.06^{Cb}	3.94 ± 0.25^{Db}
	GSE	1.58 ± 0.03^{Aa}	1.79 ± 0.02^{Bb}	1.87 ± 0.06^{Bbc}	2.15 ± 0.11^{Cc}	2.91 ± 0.10^{Dc}
	FGG	1.58 ± 0.03^{Aa}	1.62 ± 0.05^{Ac}	1.73 ± 0.05^{Bc}	1.89 ± 0.08^{Cd}	2.39 ± 0.07^{Dd}
Histamine	Control	n.d.	0.45 ± 0.03^{Aa}	1.28 ± 0.02^{Ba}	2.42 ± 0.19^{Ca}	2.76 ± 0.25^{Da}
	FG	n.d.	0.28 ± 0.06^{Ab}	0.98 ± 0.11^{Bb}	1.96 ± 0.02^{Cb}	2.45 ± 0.16^{Db}
	GSE	n.d.	0.21 ± 0.02^{Ab}	0.61 ± 0.06^{Bc}	1.02 ± 0.06^{Cc}	1.43 ± 0.02^{Dc}
	FGG	n.d.	n.d.	0.32 ± 0.04^{Ad}	0.54 ± 0.07^{Bd}	0.89 ± 0.09^{Cd}
Tyramine	Control	2.03 ± 0.22^{Aa}	2.28 ± 0.10^{Ba}	2.60 ± 0.13^{Ca}	2.90 ± 0.07 ^{Da}	3.23 ± 0.10^{Ea}
	FG	2.03 ± 0.22^{Aa}	2.12 ± 0.05^{ABb}	2.20 ± 0.02^{ABbc}	2.33 ± 0.10^{Bbc}	2.99 ± 0.20^{Cb}
	GSE	2.03 ± 0.22^{Aa}	2.14 ± 0.04^{ABb}	2.28 ± 0.05^{BCb}	2.42 ± 0.06^{CDb}	2.51 ± 0.02^{Dc}
	FGG	2.03 ± 0.22^{Aa}	2.06 ± 0.02^{Ab}	2.12 ± 0.05^{ABc}	2.23 ± 0.05^{ABc}	2.31 ± 0.08^{Bc}
Spermidine	Control	3.50 ± 0.21^{Aa}	3.30 ± 0.06^{ABa}	3.14 ± 0.08^{Ba}	2.55 ± 0.08^{Ca}	1.08 ± 0.08^{Da}
	FG	3.50 ± 0.21^{Aa}	3.40 ± 0.11^{ABab}	3.26 ± 0.05^{Bab}	3.01 ± 0.03^{Cb}	1.99 ± 0.12^{Db}
	GSE	3.50 ± 0.21^{Aa}	3.54 ± 0.08^{Abc}	3.42 ± 0.14^{Abc}	3.10 ± 0.04^{Bbc}	2.10 ± 0.15^{Cb}
	FGG	3.50 ± 0.21^{Aa}	3.56 ± 0.04^{Ac}	3.47 ± 0.04^{Ac}	3.18 ± 0.02^{Bc}	3.08 ± 0.06^{Bc}
Spermine	Control	1.69 ± 0.03^{Aa}	1.29 ± 0.09^{Ba}	1.09 ± 0.02^{Ca}	0.69 ± 0.07 ^{Da}	0.42 ± 0.04^{Ea}
	FG	1.69 ± 0.03^{Aa}	1.31 ± 0.05^{Ba}	1.19 ± 0.07^{Ca}	1.07 ± 0.02^{Db}	0.78 ± 0.04^{Eb}
	GSE	1.69 ± 0.03^{Aa}	1.52 ± 0.04^{Bb}	1.40 ± 0.11^{Bb}	1.12 ± 0.03^{Cb}	1.09 ± 0.10^{Cc}

(*continued on next page*)

Table 2 (*continued*)

Biogenic amine (mg/kg)	Treatment	Storage time (day)				
		0	3	6	9	12
	FGG	1.69 ± 0.03^{Aa}	1.68 ± 0.04^{Ac}	1.70 ± 0.03^{Ac}	1.69 ± 0.01^{Ac}	1.59 ± 0.01^{Bd}

Notes: FG: fish gelatin; GSE: grape seed extract; FGG: the combination of FG and GSE. Values with different lowercase letters at the same time point and uppercase letters of the same group indicate significant differences ($P < 0.05$), respectively. n.d., not detected.

(e.g., GSE, pomegranate peel extract) on colour qualities of fish fillets have been pointed out (Cao et al., 2020; Li et al., 2020; Zhuang et al., 2019). During storage, the L* and a* value of the control group decreased significantly while the b* value experienced a notable increased change as storage process progressed ($P < 0.05$). The changing tendencies of L*, a*, and b* values in FG, GSE and FGG groups were consistent with the control group. However, treatments with GSE alone or combined FG and GSE prohibited such tendencies efficiently, thus retarding the discoloration of seabass fillet.

A more interesting and noteworthy finding was that the FGG treatment resulted in the lowest level of ΔE in the mid to late stage of storage which meant that the colour quality of FGG-treated samples was more close to the fresh state. This result suggested colour-protection ability of FGG (Zhao, Chen, Zhao, He, & Yang, 2020). As reported, coloured components were usually generated by the protein oxidation and degradation (Zhuang et al., 2019). Thus, the colour-protection effect could be due to the cooperation of antimicrobial and antioxidant ability of GSE as well as the barrier property of FG (Cao et al., 2020; Zhao et al., 2019). Overall, FG-based coating containing GSE postponed the discoloration of seabass fillets during chilled storage.

3.5. Schematic illustration

Based on the present results, a schematic illustration of the preservative mechanism of FGG coating on seabass fillets during storage was proposed (Fig. 4). First of all, GSE (major components: proanthocyanidin and gallic acid) showed admirable antimicrobial effect against spoilage bacteria *Pseudomonas*, followed by *Aeromonas* and *Shewanella*. As detected, the total phenolic compounds in FGG coating solution was 0.45 mg gallic acid equivalent/mL (data not shown). These phenolic components in GSE could destroy the cell membrane integrity by interaction with membrane proteins, increasing the membrane permeability to cause leakage of biomaromolecules and critical ions as well as disrupting those vital bacterial metabolisms (Olatunde & Benjakul, 2018; Zhao, Chen, Wu, He, & Yang, 2020). The different susceptibility of various spoilage bacteria to GSE could due to their different cell structures. Such inhibitory effect greatly changed the bacterial composition and delayed the seabass spoilage caused by this dominant spoilage flora. Subsequently, the supressed growth of *Pseudomonas*, *Aeromonas* and *Shewanella* further inhibited the accumulation of putrescine, cadaverine and histamine in FGG-treated seabass fillets. Secondly, FG helped preserve seabass quality by acting as a gas/water barrier and inhibiting the transformation from immobilised water trapped in myofibrillar protein network to free water which was responsible for the moisture loss during seabass storage.

Lastly, the preservative effect of FGG was contributed to the synergism between GSE and FG which improved their respective properties. On the one hand, by incorporation GSE into FG-based coating, GSE could be released gradually from FG-film to perform its active functions in targeted fish flesh during the prolonged storage period. This strategy has been widely applied to improve the stability of plant extracts in food system (Jridi et al., 2015; Zhao et al., 2019). On the other hand, the addition of GSE also helped to improve the functional properties of FG through FG-GSE cross-linking network (Huang et al., 2019). In order to validate the structure modification as proposed in the schematic model (Fig. 4), FTIR analysis was conducted to illustrate the cross-linking behaviour between FG and GSE. As observed in Fig. S1, the FTIR spectra of FG and FGG samples presented similar peaks and bands of amide A, amide I, amide II, and amide III, although with slight differences in the location of the peaks. The spectra of GSE was different from those of FG and FGG at wavenumber < 1700 cm^{-1}. FGG showed modifications by GSE, in which amide A was shifted to a high wavenumber

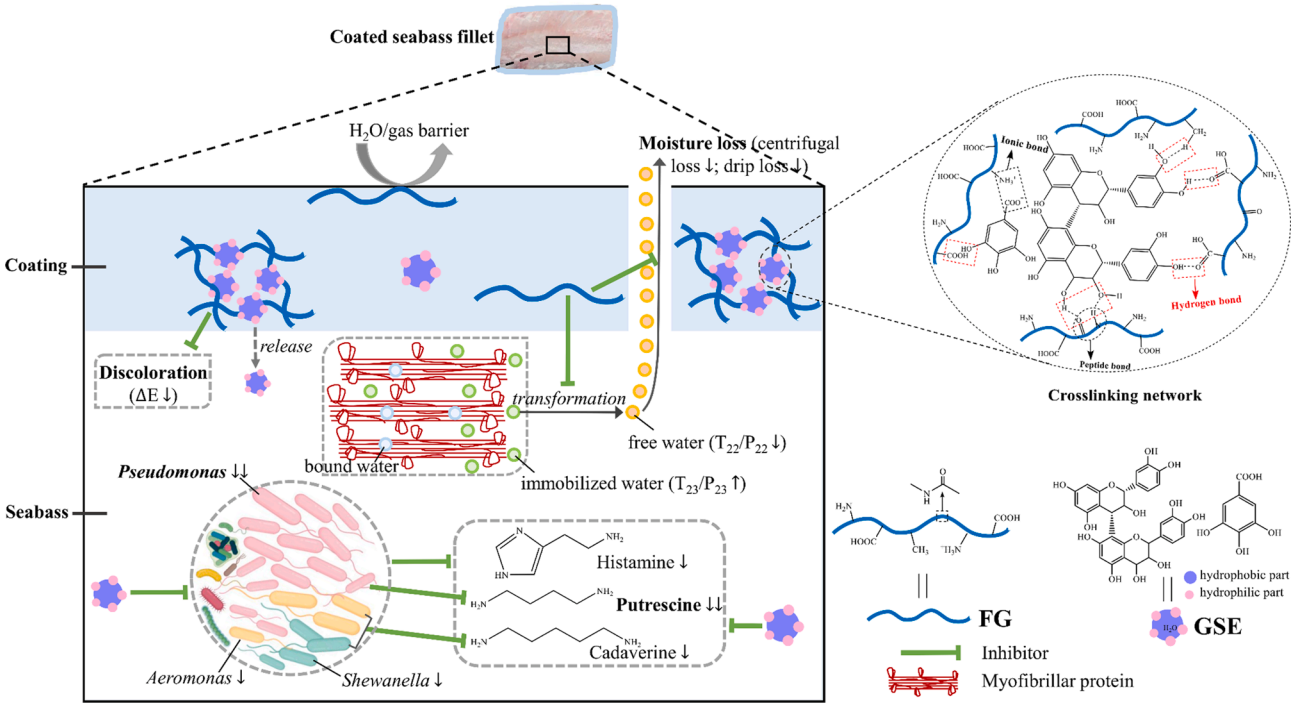

Fig 4. Schematic mechanism of the effect of fish gelatin (FG)-based coating incorporated with grape seed extract (GSE) on seabass fillets during storage.

(3285–3476 cm^{-1}) towards the O—H stretch peak of GSE (3389 cm^{-1}). This shift indicated intermolecular hydrogen bond formation between hydroxyl groups of phenolic compounds in GSE and carboxyl groups of FG (Sow, Toh, Wong, & Yang, 2019). Clearly, FGG behaved similarly to FG, while it also had characteristics of GSE. For example, there was characteristic peak at 1033 cm^{-1} in FGG corresponding to the C—H vibration on the benzene ring near the phenol –OH groups of GSE and this peak was absent in FG. Ionic bound might be formed between COO^{-} ion from phenolic acid and NH^{3+} ion of FG while the hydrophobic interaction might take place between the hydrophobic side-chain of FG and aromatic rings of GSE (Kaewdang & Benjakul, 2015; Tie, Zhang, Wang, Song, & Tan, 2020). These interactions collectively modified and offset the limitation of FG in application. To sum up, when seabass fillet was treated with FG-based coating enriched with GSE, its quality was simultaneously influenced by FG, GSE and their interactions.

4. Conclusion

FG-based coating containing GSE introduced by VI was proved to be effective in maintaining the freshness and safety of seabass fillets during 12-day chilled storage. FGG was effective in maintaining the water holding capacity by restricting water dynamics and distribution in refrigerated seabass and this mainly owed to FG. Moreover, FGG delayed the spoilage of seabass fillets by inhibiting the proliferation of spoilage microbiota. Results of high throughput sequencing and microbial enumeration further demonstrated that FGG changed the microbiota composition in seabass fillets significantly ($P < 0.05$) and inhibited the growth and multiply of *Pseudomonas*, *Aeromonas* and H_2S producing bacteria by 0.87–1.88 log CFU/g as compared to the control group. The inhibited growth of spoilage bacteria further reduced the accumulation of biogenic amines, especially putrescine and cadaverine by 59.18% and 51.03%, respectively. Lastly, it is interesting to note that FGG-treatment was effective in postponing the discoloration of seabass fillets during chilled storage. To conclude, the present work showed that FGG had the potential to serve as an active edible coating by the joint actions of FG in sustaining water holding capacity and GSE in inhibiting the survival of spoilage bacteria. In the future, application of natural edible coating may become a trend since it meet consumers' growing preferences for safe, high-quality and clean-labelled foods.

CRediT authorship contribution statement

Xue Zhao: Conceptualization, Methodology, Investigation, Software, Visualization, Writing - original draft. **Lin Chen:** Methodology, Software, Resources, Validation. **Wanwisa Wongmaneepratip:** Methodology. **Yun He:** Writing - review & editing. **Lin Zhao:** Writing - review & editing. **Hongshun Yang:** Conceptualization, Funding acquisition, Project administration, Supervision, Writing - review & editing.

Declaration of Competing Interest

The authors declare that they have no known competing financial interests or personal relationships that could have appeared to influence the work reported in this paper.

Acknowledgements

The authors acknowledge the financial support by Singapore Ministry of Education Academic Research Fund Tier 1 (R-160-000-A40-114), Applied Basic Research Project (Agricultural) Suzhou Science and Technology Planning Programme (SYN2020061), Natural Science Foundation of Jiangsu Province (BK20181184), and an industry project (R-160-000-A21-597) from Shanghai ProfLeader Biotech Co., Ltd.

Appendix A. Supplementary data

Supplementary data to this article can be found online at https://doi.org/10.1016/j.foodchem.2021.129581.

References

Albertos, I., Martin-Diana, A. B., Cullen, P. J., Tiwari, B. K., Ojha, K. S., Bourke, P., & Rico, D. (2019). Shelf-life extension of herring (*Clupea harengus*) using in-package atmospheric plasma technology. *Innovative Food Science & Emerging Technologies, 53*, 85–91.

Arfat, Y. A., Benjakul, S., Vongkamjan, K., Sumpavapol, P., & Yarnpakdee, S. (2015). Shelf-life extension of refrigerated sea bass slices wrapped with fish protein isolate/fish skin gelatin-ZnO nanocomposite film incorporated with basil leaf essential oil. *Journal of Food Science and Technology, 52*(10), 6182–6193.

Bertram, H. C., Purslow, P. P., & Andersen, H. J. (2002). Relationship between meat structure, water mobility, and distribution: A low-field nuclear magnetic resonance study. *Journal of Agricultural and Food Chemistry, 50*(4), 824–829.

Biji, K. B., Ravishankar, C. N., Venkateswarlu, R., Mohan, C. O., & Gopal, T. K. S. (2016). Biogenic amines in seafood: A review. *Journal of Food Science and Technology, 53*(5), 2210–2218.

Cao, J., Wang, Q.i., Ma, T., Bao, K., Yu, X., Duan, Z., … Li, C. (2020). Effect of EGCG-gelatin biofilm on the quality and microbial composition of tilapia fillets during chilled storage. *Food Chemistry, 305*, 125454. https://doi.org/10.1016/j.foodchem.2019.125454.

Cao, L.i., Wang, J., Sun, L.u., Kong, Z., Wu, Q., & Wang, Z. (2019). Transcriptional analysis reveals the relativity of acid tolerance and antimicrobial peptide resistance of *Salmonella*. *Microbial Pathogenesis, 136*, 103701. https://doi.org/10.1016/j.micpath.2019.103701.

Chaijan, S., Panpipat, W., Panya, A., Cheong, L.-Z., & Chaijan, M. (2020). Preservation of chilled Asian sea bass (*Lates calcarifer*) steak by whey protein isolate coating containing polyphenol extract from ginger, lemongrass, or green tea. *Food Control, 118*, 107400. https://doi.org/10.1016/j.foodcont.2020.107400.

Fraser, O. P., & Sumar, S. (1998). Compositional changes and spoilage in fish (part II)-microbiological induced deterioration. *Nutrition & Food Science, 98*(6), 325–329.

Nur Hanani, Z. A., Roos, Y. H., & Kerry, J. P. (2012). Use of beef, pork and fish gelatin sources in the manufacture of films and assessment of their composition and mechanical properties. *Food Hydrocolloids, 29*(1), 144–151.

Huang, T., Tu, Z.-C., Shangguan, X., Sha, X., Wang, H., Zhang, L.u., & Bansal, N. (2019). Fish gelatin modifications: A comprehensive review. *Trends in Food Science & Technology, 86*, 260–269.

Jia, S., Li, Y., Zhuang, S., Sun, X., Zhang, L., Shi, J., … Luo, Y. (2019). Biochemical changes induced by dominant bacteria in chill-stored silver carp (*Hypophthalmichthys molitrix*) and GC-IMS identification of volatile organic compounds. *Food Microbiology, 84*, 103248. https://doi.org/10.1016/j.fm.2019.103248.

Jridi, M., Abdelhedi, O., Souissi, N., Kammoun, M., Nasri, M., & Ayadi, M. (2015). Improvement of the physicochemical, textural and sensory properties of meat sausage by edible cuttlefish gelatin addition. *Food Bioscience, 12*, 67–72.

Ju, J., Xie, Y., Guo, Y., Cheng, Y., Qian, H.e., & Yao, W. (2019). Application of edible coating with essential oil in food preservation. *Critical Reviews in Food Science and Nutrition, 59*(15), 2467–2480.

Kaewdang, O., & Benjakul, S. (2015). Effect of ethanolic extract of coconut husk on gel properties of gelatin from swim bladder of yellowfin tuna. *LWT-Food Science and Technology, 62*(2), 955–961.

Latorre-Moratalla, M. L., Bover-Cid, S., Bosch-Fusté, J., Veciana-Nogués, M. T., & Vidal-Carou, M. C. (2014). Amino acid availability as an influential factor on the biogenic amine formation in dry fermented sausages. *Food Control, 36*(1), 76–81.

Lázaro, C. A., Monteiro, M. L. G., & Conte-Junior, C. A. (2020). Combined effect of modified atmosphere packaging and UV-C radiation on pathogens reduction, biogenic amines, and shelf life of refrigerated tilapia (*Oreochromis niloticus*) fillets. *Molecules, 25*(14), 3222.

Li, M., Li, B., & Zhang, W. (2018). Rapid and non-invasive detection and imaging of the hydrocolloid-injected prawns with low-field NMR and MRI. *Food Chemistry, 242*, 16–21.

Li, P., Peng, Y., Mei, J., & Xie, J. (2020). Effects of microencapsulated eugenol emulsions on microbiological, chemical and organoleptic qualities of farmed Japanese sea bass (*Lateolabrax japonicus*) during cold storage. *LWT-Food Science and Technology, 118*, 108831. https://doi.org/10.1016/j.lwt.2019.108831.

Li, Y., Zhuang, S., Liu, Y., Zhang, L., Liu, X., Cheng, H., … Luo, Y. (2020). Effect of grape seed extract on quality and microbiota community of container-cultured snakehead (*Channa argus*) fillets during chilled storage. *Food Microbiology, 91*, 103492. https://doi.org/10.1016/j.fm.2020.103492.

Lou, X., Zhai, D., & Yang, H. (2021). Changes of metabolite profiles of fish models inoculated with *Shewanella baltica* during spoilage. *Food Control, 123*, 107697. https://doi.org/10.1016/j.foodcont.2020.107697.

Memar, M. Y., Adibkia, K., Farajnia, S., Kafil, H. S., Yekani, M., Alizadeh, N., & Ghotaslou, R. (2019). The grape seed extract: A natural antimicrobial agent against different pathogens. *Reviews in Medical Microbiology, 30*(3), 173–182.

Nian, L., Cao, A., Cai, L., Ji, H., & Liu, S. (2019). Effect of vacuum impregnation of red sea bream (*Pagrosomus major*) with herring AFP combined with CS@Fe3O4 nanoparticles during freeze-thaw cycles. *Food Chemistry, 291*, 139–148.

Olatunde, O. O., & Benjakul, S. (2018). Natural preservatives for extending the shelf-life of seafood: A revisit. *Comprehensive Reviews in Food Science and Food Safety, 17*(6), 1595–1612.

Pearce, K. L., Rosenvold, K., Andersen, H. J., & Hopkins, D. L. (2011). Water distribution and mobility in meat during the conversion of muscle to meat and ageing and the impacts on fresh meat quality attributes–A review. *Meat Science, 89*(2), 111–124.

Sow, L. C., Toh, N. Z. Y., Wong, C. W., & Yang, H. (2019). Combination of sodium alginate with tilapia fish gelatin for improved texture properties and nanostructure modification. *Food Hydrocolloids, 94*, 459–467.

Syropoulou, F., Parlapani, F. F., Bosmali, I., Madesis, P., & Boziaris, I. S. (2020). HRM and 16S rRNA gene sequencing reveal the cultivable microbiota of the European sea bass during ice storage. *International Journal of Food Microbiology, 327*, 108658. https://doi.org/10.1016/j.ijfoodmicro.2020.108658.

Tie, S., Zhang, X., Wang, H., Song, Y., & Tan, M. (2020). Procyanidins-loaded complex coacervates for improved stability by self-crosslinking and calcium ions chelation. *Journal of Agricultural and Food Chemistry, 68*(10), 3163–3170.

Visciano, P., Schirone, M., Tofalo, R., & Suzzi, G. (2012). Biogenic amines in raw and processed seafood. *Frontiers in Microbiology, 3*, 188.

Yılmaz, F. M., & Ersus Bilek, S. (2018). Ultrasound-assisted vacuum impregnation on the fortification of fresh-cut apple with calcium and black carrot phenolics. *Ultrasonics Sonochemistry, 48*, 509–516.

Yu, D., Wu, L., Regenstein, J. M., Jiang, Q., Yang, F., Xu, Y., & Xia, W. (2020). Recent advances in quality retention of non-frozen fish and fishery products: A review. *Critical Reviews in Food Science and Nutrition, 60*(10), 1747–1759.

Zhang, L., Li, Q., Lyu, J., Kong, C., Song, S., & Luo, Y. (2017). The impact of stunning methods on stress conditions and quality of silver carp (*Hypophthalmichthys molitrix*) fillets stored at 4 °C during 72 h postmortem. *Food Chemistry, 216*, 130–137.

Zhang, L., Zhang, Y., Jia, S., Li, Y., Li, Q., Li, K., … Luo, Y. (2019). Stunning stress-induced textural softening in silver carp (*Hypophthalmichthys molitrix*) fillets and underlying mechanisms. *Food Chemistry, 295*, 520–529.

Zhang, X., & Xie, J. (2019). Analysis of proteins associated with quality deterioration of grouper fillets based on TMT quantitative proteomics during refrigerated storage. *Molecules, 24*(14), 2641.

Zhao, X., Chen, L., Wu, Ji'en, He, Y., & Yang, H. (2020). Elucidating antimicrobial mechanism of nisin and grape seed extract against *Listeria monocytogenes* in broth and on shrimp through NMR-based metabolomics approach. *International Journal of Food Microbiology, 319*, 108494. https://doi.org/10.1016/j.ijfoodmicro.2019.108494.

Zhao, X., Chen, L., Zhao, L., He, Y., & Yang, H. (2020). Antimicrobial kinetics of nisin and grape seed extract against inoculated *Listeria monocytogenes* on cooked shrimp: Survival and residual effects. *Food Control, 107278*.

Zhao, X., Wu, Ji'en, Chen, L., & Yang, H. (2019). Effect of vacuum impregnated fish gelatin and grape seed extract on metabolite profiles of tilapia (*Oreochromis niloticus*) fillets during storage. *Food Chemistry, 293*, 418–428.

Zhao, X., Zhou, Y., Zhao, L., Chen, L., He, Y., & Yang, H. (2019). Vacuum impregnation of fish gelatin combined with grape seed extract inhibits protein oxidation and degradation of chilled tilapia fillets. *Food Chemistry, 294*, 316–325.

Zhao, Y.-M., de Alba, M., Sun, D.-W., & Tiwari, B. (2019). Principles and recent applications of novel non-thermal processing technologies for the fish industry−A review. *Critical Reviews in Food Science and Nutrition, 59*(5), 728–742.

Zhou, Q., Li, P., Fang, S., Mei, J., & Xie, J. (2020). Preservative effects of gelatin active coating containing eugenol and higher CO_2 concentration modified atmosphere packaging on Chinese sea bass (*Lateolabrax maculatus*) during superchilling (−0.9 °C) storage. *Molecules, 25*(4), 871.

Zhuang, S., Li, Y., Jia, S., Hong, H., Liu, Y., & Luo, Y. (2019). Effects of pomegranate peel extract on quality and microbiota composition of bighead carp (*Aristichthys nobilis*) fillets during chilled storage. *Food Microbiology, 82*, 445–454.